Bulgarian Journal of Meteorology & Hydrology, vol. 5 (1994). 105–118.

Numerical Investigation of High–Re Stationary Viscous Flow around Circular Cylinder as Inverse Problem

C. I. Christov *
Centre for Nonlinear Phenomena and Complex Systems, Université Libre de Bruxelles, Campus Plaine - CP231, Bruxelles 1050, BELGIQUE

R. Marinova
Dept. of Mathematics, Technical University of Varna, Varna, 9010, BULGARIA

The steady viscous flow around circular cylinder is considered for Reynolds numbers for which it is unstable. Method of Variational Imbedding is applied which replaces the original problem by higher–order correct boundary value problem. The latter is solved numerically by a difference scheme of splitting type. Results are obtained in the range $0 \leq Re \leq 100$ and shown to be in good agreement with the literature.

Рассматривается стационарное вязкое течение вокруг кругового цилиндра при чисел Рейнолдса для которых оно неустойчиво. Применяется Метод Вариационного Погружения, в котором изходная граничная задача заменяется коректной задачей более высокого порядка. Новая граничная задача решается числено методом дробных шагов. Получены результаты в интервале $0 \leq Re \leq 100$ которые находятся в хорошем согласии с результатыми других авторов.

1. Introduction

One of the most important traits of Navier-Stokes equations (N–S for brevity) is that for large Reynolds numbers their solutions become unstable and through different kinds of bifurcations the flow ends up eventually in a turbulent regime. Various scenarios of transition are known: linear bifurcation with multitude of secondary stationary regimes in Taylor-Cuette flow, stiff bifurcation with explosion of a chaotic regime in Poiseuille flow, etc. The essential problem everywhere is the same: for sufficiently large Reynolds number the stationary laminar solution can not be obtained as an initial value problem, i.e., the problem of finding the stationary solution becomes incorrect in the sense of Hadamard.

At the same time it is very important to know the pattern of the steady flow at high Reynolds numbers (even in the parametric domains where it is instable) for investigating the asymptotic properties of N–S, especially the asymptotics of the wake, points of detachment of the flow on the cylinder, pressure distribution alongside the cylinder surface, etc.

Of fundamental importance is to answer the question of whether the stationary solution still exists for higher Reynolds numbers or it eventually disappears because this characterizes N–

*On leave from National Institute of Meteorology & Hydrology, Bulgarian Academy of Sciences, Sofia 1184, BULGARIA

S as a dynamical system. Using the language of theory of dynamical systems, the question is whether the stationary points of the system (here: in the sense of functional space) disappear after ceasing to attract the trajectories or they do persist without attracting the solution. To these questions the answers can be provided only by solving the incorrect problem.

The numerical value of critical Reynolds number for transition depends on flow geometry. In the present work the steady flow past a circular cylinder is considered as a typical example of a flow that becomes unstable as early as $Re = 40$ (Reynolds number based on the diameter of the cylinder). For larger $40 < Re < 100$ the stationary regime is replaced by an unsteady laminar flow called "Kármán vortex street". With further increase of Re the flow ends up in the turbulent regime. There exist in the literature a number of numerical solutions to the stationary problem for $Re > 40$ and all of them explicitly or implicitly make use of smoothing techniques in order to filter out the disturbances that lead to change to unsteady regime. The purpose of the present work is to follow radically different way and to treat the problem as inverse one. To this end we employ a technique called Method of Variational Imbedding. Some preliminary results obtained along these lines were announced in [18].

2. High Reynolds Number Flow past a Circular Cylinder

2.1. Posing the Problem

In polar coordinates, the dimensionless steady Navier-Stokes and continuity equations have the form

$$u_r\frac{\partial u_\varphi}{\partial r} + \frac{u_\varphi}{r}\frac{\partial u_\varphi}{\partial \varphi} + \frac{u_\varphi u_r}{r} = -\frac{1}{r}\frac{\partial p}{\partial \varphi} + \frac{1}{Re}\left[Du_\varphi + \frac{2}{r}\frac{\partial u_r}{\partial \varphi}\right], \qquad (2.1)$$

$$u_r\frac{\partial u_r}{\partial r} + \frac{u_\varphi}{r}\frac{\partial u_r}{\partial \varphi} - \frac{u_\varphi^2}{r} = -\frac{\partial p}{\partial r} + \frac{1}{Re}\left[Du_r - \frac{2}{r}\frac{\partial u_\varphi}{\partial \varphi}\right], \qquad (2.2)$$

$$\frac{\partial u_r}{\partial r} + \frac{u_r}{r} + \frac{1}{r}\frac{\partial u_\varphi}{\partial \varphi} = 0\,, \qquad (2.3)$$

where $u_r = u(r,\varphi)$ and $u_\varphi = v(r,\varphi)$ are the velocity components parallel respectively to the polar axes r and φ; and $p = p(x,y)$ is the pressure. Respectively,

$$D \equiv \frac{\partial^2}{\partial r^2} + \frac{1}{r}\frac{\partial}{\partial r} - \frac{1}{r^2} + \frac{1}{r^2}\frac{\partial^2}{\partial \varphi^2}$$

is called *Stokesian.*

The Reynolds number $Re = dU_\infty/\nu$ is the governing dimensionless parameter. The cylinder diameter $d = 2a$ is the characteristic length; velocity at infinity U_∞ is the characteristic velocity; and ν is the kinematic coefficient of viscosity. In terms of dimensionless variables, the cylinder surface is represented by $r = 1$ while the velocity at infinity – by unity.

The boundary conditions (b.c. – for brevity) reflect the non-slipping at the cylinder surface

$$u_r(1,\varphi) = u_\varphi(1,\varphi) = 0\,. \qquad (2.4)$$

on the one hand, and the asymptotic matching with the uniform outer flow at infinity – on the other. Numerically one has to pose the asymptotic condition at certain large enough value of the radial coordinate called "actual infinity", say R_∞. Then the dimensionless b.c. read

$$\begin{aligned} u_r(R_\infty,\varphi) &= \cos\varphi\,, \\ u_\varphi(R_\infty,\varphi) &= -\sin\varphi\,. \end{aligned} \qquad (2.5)$$

Due to the obvious flow symmetry with respect to the line $\varphi = 0, \pi$, the computational domain may be reduced to $0 \le \varphi \le \pi$, $r \ge 1$ and additional b.c. on the lines $\varphi = 0$ and $\varphi = \pi$, are added to acknowledge the mentioned symmetry, namely

$$\begin{aligned} u_\varphi(r,0) &= 0\,, \quad \left.\frac{\partial u_r}{\partial \varphi}\right|_{(r,0)} = 0\,, \\ u_\varphi(r,\pi) &= 0\,, \quad \left.\frac{\partial u_r}{\partial \varphi}\right|_{(r,\pi)} = 0\,, \end{aligned} \qquad (2.6)$$

2.2. Numerical difficulties for Large Reynolds Numbers

The flow past a circular cylinder poses some special problems when devising the difference scheme and algorithms. The worst is a result from the unboundedness of the flow and the slow algebraic decay $\sim r^{-1}$ of the solution at infinity. The latter leaves the door open for different kinds of errors connected with the so–called "actual infinity". On the other hand, neither cartesian nor polar coordinate systems are adequate enough for describing the topology of the flow when the separation takes place. These problems are aggravated with the increase of Reynolds number. The conformal mapping as the one employed by Fornberg [12,13] do improve the topological fitness of the mesh but on the expense of introducing artificial singularities at the boundary of the body. Another possibility is to use parabolic coordinate as done in [9,8] for ideal separated flows. In this first work on MVI for N–S we refrain from more complicated meshes in order to concentrate on the basic features of the approach.

Table 1 is the table from Fornberg's works completed with his own results and those of Patel [21]. It shows the development of numerical techniques for the stationary and non-stationary flows past cylinders. Most of authors used the vorticity/ stream function formulation. The first solution is already classics of CFD – this is the Thom's solution from 1933. Most of the solutions remain in the region of $Re < 100$ which is natural in the light of what has been above said about the instability of the stationary solution. Only Fornberg [12,13] decisively improved the range of applicability of the numerical approach but once again on the expense of applying smoothing which although instrumental can not be rigorously justified.

Table 1: Some known computations from the literature

Work	Re	R_∞
Thom, 1933 [26]	20	
Kawaguti, 1953 [16]	40	
Jain & Kawaguti, 1966 [14]	50	111
Keller & Takami, 1966 [17]	15	59
Jain & Sankara Rao, 1969 [15]	40	111
Son & Hanratty, 1969 [23]	40	157
Takami & Keller, 1969 [25]	60	17
Thoman & Szewczyk, 1969 [27]	30	18
Underwood, 1969 [29]	10	40
Dennis & Chang, 1970 [11]	100	39
Nieuwstadt & Keller, 1973 [20]	40	23
Ta, 1975 [24]	120	36
Tuann & Olson, 1978 [28]	100	20
Fornberg, 1980 [12]	300	600
Fornberg, 1985 [13]	600	600
Patel, 1987 [21]	40	103

3. Method of Variational Imbedding (MVI)

Recently the so-called Method of Variational Imbedding (MVI – for brevity) has been developed [1,2,3,4] for inverse and incorrect problems. MVI is a specific implementation of the Least Square Method to ODE and PDE and the gist is to replace the direct solution of the "stiff" (unstable, incorrect, etc.) boundary or initial value problem with the problem of minimization of the quadratic functional of the original set of equations. The necessary conditions for the minimization of a functional yield to an apparently more complicated Euler-Lagrange system to whose solution(s) belongs also the solution of the original incorrect problem. The advantage is that the imbedding system is much more tractable and its stationary solutions are stable, because it has very little in common with the original physically unstable system. Thus the solution of the original system is "imbedded" into the solutions of some other system through a variational procedure - here comes the coinage MVI. Only for linear problems, the Euler–Lagrange equations possess unique solution and then there is one–to–one correspondence between the original and variational problems and one may not speak about imbedding. In the general case, however, the E–L equations possess more than one solution, corresponding

to different local extrema, and only the solution on which the minimum of the functional is zero is the solution of the original problem.

Consider the Imbedding functional

$$\mathcal{J} = \int_0^{\pi} \int_1^{\infty} \left(\Phi^2 + \Omega^2 + X^2\right) r dr d\varphi, \quad (3.1)$$

where:

$$\begin{aligned}
\Phi &= u_r \frac{\partial u_\varphi}{\partial r} + \frac{u_\varphi}{r}\frac{\partial u_\varphi}{\partial \varphi} + \frac{u_\varphi u_r}{r} + \frac{1}{r}\frac{\partial p}{\partial \varphi} \\
&- \frac{1}{Re}\left(Du_\varphi + \frac{2}{r^2}\frac{\partial u_r}{\partial \varphi}\right) \\
\Omega &= u_r \frac{\partial u_r}{\partial r} + \frac{u_\varphi}{r}\frac{\partial u_r}{\partial \varphi} - \frac{u_\varphi^2}{r} + \frac{\partial p}{\partial r} \\
&- \frac{1}{Re}\left(Du_r - \frac{2}{r^2}\frac{\partial u_\varphi}{\partial \varphi}\right) \\
X &= \frac{\partial u_r}{\partial r} + \frac{u_r}{r} + \frac{1}{r}\frac{\partial u_\varphi}{\partial \varphi}
\end{aligned}$$

As far as the boundary value problem for the N–S equations possesses a solution then the global minimum of the functional (3.1) is equal to zero which is the value the functional assumes on the solutions of N–S. This allows us to seek for a local minimum of the functional $\mathcal{J}$ and to check afterwards whether this is the global minimum.

The necessary conditions for minimizing of a functional are the so–called Euler–Lagrange equations which in the case under consideration have the form

$$\begin{aligned}
\frac{\partial F}{\partial u_r} &- \frac{d}{d\varphi}\left(\frac{\partial F}{\partial \frac{\partial u_r}{\partial \varphi}}\right) - \frac{d}{dr}\left(\frac{\partial F}{\partial \frac{\partial u_r}{\partial r}}\right) \quad (3.2) \\
&+ \frac{d^2}{d\varphi^2}\left(\frac{\partial F}{\partial \frac{\partial^2 u_r}{\partial \varphi^2}}\right) + \frac{d^2}{dr^2}\left(\frac{\partial F}{\partial \frac{\partial^2 u_r}{\partial r^2}}\right) = 0,
\end{aligned}$$

$$\begin{aligned}
\frac{\partial F}{\partial u_\varphi} &- \frac{d}{d\varphi}\left(\frac{\partial F}{\partial \frac{\partial u_\varphi}{\partial \varphi}}\right) - \frac{d}{dr}\left(\frac{\partial F}{\partial \frac{\partial u_\varphi}{\partial r}}\right) \quad (3.3) \\
&+ \frac{d^2}{d\varphi^2}\left(\frac{\partial F}{\partial \frac{\partial^2 u_\varphi}{\partial \varphi^2}}\right) + \frac{d^2}{dr^2}\left(\frac{\partial F}{\partial \frac{\partial^2 u_\varphi}{\partial r^2}}\right) = 0,
\end{aligned}$$

where $F = (\Phi^2 + \Omega^2 + X^2)$.

In details the Euler-Lagrange equations are presented in the Appendix.

Equations (8.1) and (8.2) are of fourth order and (8.3) – of second order. All three of them are of elliptic type and one can consider the set of imbedding equations as elliptic system of tenth order. The new system looks apparently much more complicated than the original, but in fact what counts is the well posedness of the boundary value problem.

The increased order of the system requires larger number of boundary conditions. They are obtained form the so-called "natural" conditions for minimization of a functional. In the case under consideration they are simply the original equations taken at the boundary, namely

$$\begin{aligned}
\Phi(1,\varphi) = 0\,, \quad \Phi(R_\infty,\varphi) = 0\,, \\
\Phi(r,0) = 0\,, \quad \Phi(r,\pi) = 0\,, \\
\Omega(1,\varphi) = 0\,, \quad \Omega(R_\infty,\varphi) = 0\,, \\
\Omega(r,0) = 0\,, \quad \Omega(r,\pi) = 0\,, \\
X(1,\varphi) = 0\,, \quad X(R_\infty,\varphi) = 0\,, \\
X(r,0) = 0\,, \quad X(r,\pi) = 0\,,
\end{aligned}$$

These conditions together with the eight conditions (2.4), (2.6) on velocity components give the necessary twenty b.c. for the imbedding system.

After some obvious manipulations we arrive at the following b.c. for the three sought functions

$$\begin{aligned}
u_\varphi(1,\varphi) = u_r(1,\varphi) = \left.\frac{\partial u_r}{\partial r}\right|_{r=1} &= 0\,, \\
\left[\frac{1}{Re}\frac{\partial}{\partial r} r \frac{\partial}{\partial r} u_\varphi - \frac{\partial p}{\partial \varphi}\right]_{r=1} &= 0\,, \quad (3.4)
\end{aligned}$$

$$\begin{aligned}
u_\varphi(R_\infty,\varphi) = -\sin\varphi\,, \quad u_r(R_\infty,\varphi) &= \cos\varphi\,, \\
\left.\frac{\partial u_r}{\partial r}\right|_{r=R_\infty} = \left.\frac{\partial u_\varphi}{\partial r}\right|_{r=R_\infty} &= 0\,, \quad (3.5)
\end{aligned}$$

$$u_\varphi(r,0) = \left.\frac{\partial^2 u_\varphi}{\partial \varphi^2}\right|_{\varphi=0} = \left.\frac{\partial u_r}{\partial \varphi}\right|_{\varphi=0} = 0\,, \quad (3.6)$$

$$u_\varphi(r,\pi) = \left.\frac{\partial^2 u_\varphi}{\partial \varphi^2}\right|_{\varphi=\pi} = \left.\frac{\partial u_r}{\partial \varphi}\right|_{\varphi=\pi} = 0\,, \quad (3.7)$$

Parts of conditions (3.4),(3.5), (3.6) and (3.7) containing u_φ are b.c for equation (8.2). Respectively, the parts containing u_r are b.c for equation (8.1). Some minor problems arise when employing the conditions that are in fact the original equations, because they are of non–local form

$$u_r \frac{\partial u_r}{\partial r} + \frac{\partial p}{\partial r} - \frac{1}{Re}\left[Du_r - \frac{2}{r^2}\frac{\partial u_\varphi}{\partial \varphi}\right] = 0\,, \quad (3.8)$$

containing both normal and tangential derivatives of the sought function. In this instance some more care is needed when splitting them in the method of fractional steps (see the Section on splitting).

Finally, the b.c. for pressure read

$$\begin{aligned} \left.\frac{\partial p}{\partial r}\right|_{r=1} &= \left.\frac{1}{Re}\frac{\partial^2 u_r}{\partial r^2}\right|_{r=1}, \\ \left.\frac{\partial p}{\partial r}\right|_{r=R_\infty} &= \left.\frac{1}{Re}\frac{\partial^2 u_r}{\partial r^2}\right|_{r=R_\infty}, \quad (3.9) \\ \left.\frac{\partial p}{\partial \varphi}\right|_{\varphi=0} &= \left.\frac{\partial p}{\partial \varphi}\right|_{\varphi=\pi} = 0\,. \end{aligned}$$

4. Iterative Difference Solution to Imbedding Problem

The leading–order linear operators of the boundary value problem (b.v.p – for brevity) derived in the previous Section are of fourth order, so it may be considered as nonlinear bi–harmonic problem. It can only be solved by means of an iterational process in which at each stage the equations are linearized. The most consistent way is to use Newton's quasilinearization but it yields coupled systems of difference equations that require of order of magnitude more computational time than each of the imbedding equations. For this reason we employ the simplest linearization in which we suppose that in the coefficients of the different differential operators that enter (8.1),(8.2),(8.3), the velocity components and their derivatives are known from the previous iteration. Denote these known functions by $\hat{u}_\varphi(r,\varphi)$ and $\hat{u}_r(r,\varphi)$.

For the difference approximations of the main operators we introduce the notations:

$$\Lambda^{[\varphi]}_{4\varphi} \simeq -\frac{1}{Re^2\, r^4}\frac{\partial^4}{\partial \varphi^4} + \frac{1}{r^2}\frac{\partial}{\partial \varphi}\left(1+\hat{u}_\varphi^2\right)\frac{\partial}{\partial \varphi}\,, \quad (4.1)$$

$$\begin{aligned} \Lambda^{[\varphi]}_{4r} \simeq & -\frac{1}{Re^2}\frac{\partial^4}{\partial r^4} + \frac{\partial}{\partial r}\left[\left(\hat{u}_r - \frac{1}{Re\, r}\right)^2 \frac{\partial}{\partial r}\right] \\ & - \left(\frac{1}{r}\frac{\partial \hat{u}_r}{\partial \varphi} - \frac{\hat{u}_\varphi}{r}\right)^2 - \left(\frac{1}{r}\frac{\partial \hat{u}_\varphi}{\partial \varphi} + \frac{1}{r^2 Re}\right)^2, \quad (4.2) \end{aligned}$$

$$\begin{aligned} \Lambda^{[r]}_{4\varphi} \simeq & -\frac{1}{Re^2\, r^4}\frac{\partial^4}{\partial \varphi^4} + \frac{1}{r^2}\frac{\partial}{\partial \varphi}\hat{u}_\varphi^2\frac{\partial}{\partial \varphi} \quad (4.3) \\ & - \left(\frac{\partial \hat{u}_\varphi}{\partial r} + \frac{\hat{u}_\varphi}{r}\right)^2 - \left(\frac{\partial \hat{u}_r}{\partial r} + \frac{1}{Re\, r^2}\right)^2, \end{aligned}$$

$$\begin{aligned} \Lambda^{[r]}_{4r} \simeq & -\frac{1}{Re^2}\frac{\partial^4}{\partial r^4} + \frac{\partial^2}{\partial r^2} \\ & + \frac{\partial}{\partial r}\left[\left(\hat{u}_r - \frac{1}{Re\, r}\right)^2 \frac{\partial}{\partial r}\right], \quad (4.4) \end{aligned}$$

$$\Lambda_{\varphi\varphi} \simeq \frac{1}{r^2}\frac{\partial^2}{\partial \varphi^2}\,, \quad (4.5)$$

$$\Lambda_{rr} \simeq \frac{1}{r}\frac{\partial}{\partial^r}r\frac{\partial}{\partial r}\,, \quad (4.6)$$

Those terms of equations (8.1),(8.2) and (8.3) that are not among the specified by (4.1)–(4.6) we denote by $\mathcal{N}_{[\varphi]}, \mathcal{N}_{[r]}$ and $\mathcal{N}_{[p]}$, respectively.

4.1. The Splitting

In (8.1),(8.2) and (8.3) we add derivatives with respect to a fictitious time and render the problem to a generalized parabolic b.v.p. This has nothing in common with the physically non–stationary N–S equations and hence it does not loose stability under same conditions as N–S do.

A cost efficient algorithm for solving the "parabolized" imbedding b.v.p. can be constructed using the method of coordinate splitting pioneered in [22] (see, also [30]). The main difference here from the mentioned works is that the parabolic system contains fourth–order diffusion operators. The splitting algorithm for bi-harmonic operators was outlined in [2] and applied in [19] to boundary layer thickness iden-

tification and in [6] – to the so-called Swift-Hohenberg equation. Recently, the same idea was employed to the stationary Navier–Stokes equations [7].

We generalize the scheme of "stabilizing correction" or second Douglass scheme (see, e.g., [30]) to the nonlinear bi–harmonic b.v.p considered here.

4.1.1. Splitting for u_φ:

After introducing fictitious time, the equation for u_φ becomes a parabolic difference equation. An implicit scheme for time stepping of the solution could be the following one

$$\frac{u_\varphi^{n+1}-u_\varphi^n}{\Delta\tau}=\left(\Lambda_{4r}^{[\varphi]}+\Lambda_{4\varphi}^{[\varphi]}\right)u_\varphi^{n+1}+\mathcal{N}_{[\varphi]}^n\,, \quad (4.7)$$

where the superscript (n) stands for the current time stage and $(n+1)$ for the "new" time stage.

The above implicit scheme in full time steps is approximated by the fractional-step scheme (be reminded that $\hat{u}_\varphi \equiv u_\varphi^n$ and $\hat{u}_r \equiv u_r^n$)

$$\frac{u_\varphi^{n+\frac{1}{2}}-u_\varphi^n}{\Delta\tau} = \Lambda_{4r}^{[\varphi]}u_\varphi^{n+\frac{1}{2}}+\Lambda_{4\varphi}^{[\varphi]}u_\varphi^n+\mathcal{N}_{[\varphi]}^n\,, \quad (4.8)$$

$$\frac{u_\varphi^{n+1}-u_\varphi^{n+\frac{1}{2}}}{\Delta\tau} = \Lambda_{4\varphi}^{[\varphi]}(u_\varphi^{n+1}-u_\varphi^n)\,, \quad (4.9)$$

subjected to the respective part of boundary conditions (3.4)–(3.7). The last scheme can be rewritten as

$$(E-\Delta\tau\Lambda_{4r}^{[\varphi]})u_\varphi^{n+\frac{1}{2}} = (E-\Delta\tau\Lambda_{4\varphi}^{[\varphi]})u_\varphi^n + \Delta\tau\mathcal{N}_{[\varphi]}^n\,, \quad (4.10)$$

$$(E-\Delta\tau\Lambda_{4\varphi}^{[\varphi]})u_\varphi^{n+1} = Eu_\varphi^{n+\frac{1}{2}} - \Delta\tau\Lambda_{4\varphi}^{[\varphi]}u_\varphi^n\,, \quad (4.11)$$

where E stands for the identity difference operator.

In order to show that the splitting scheme approximates the former we exclude $u_\varphi^{n+\frac{1}{2}}$. To this end we act upon the eq.(4.11) by the operator $(E-\Delta\tau\Lambda_{4r}^{[\varphi]})$ and add the result to (4.10). After some obvious manipulations we obtain

$$\left[E+(\Delta\tau)^2\Lambda_{4r}^{[\varphi]}\Lambda_{4\varphi}^{[\varphi]}\right]\frac{u_\varphi^{n+1}-u_\varphi^n}{\Delta\tau} = \left(\Lambda_{4r}^{[\varphi]}+\Lambda_{4\varphi}^{[\varphi]}\right)u_\varphi^{n+1}+\mathcal{N}_{[\varphi]}^n\,, \quad (4.12)$$

which approximates the implicit scheme in full time steps (4.7) with $O((\Delta\tau)^2)$. One can see now that not only is the splitting scheme cost efficient, but it is also more stable than the scheme (4.7) since the operator in the l.h.s acting upon the time difference has a norm greater than unity. When inverting it one gets an operator of norm lesser than unity increasing thus stability of the scheme.

4.1.2. Splitting for u_r:

In a similar fashion we propose an implicit scheme for the equation for u_r in the form

$$\frac{u_r^{n+1}-u_r^n}{\Delta\tau}=\left(\Lambda_{4r}^{[r]}+\Lambda_{4\varphi}^{[r]}\right)u_r^{n+1}+\mathcal{N}_{[r]}^n\,, \quad (4.13)$$

which is approximated by the fractional steps

$$\frac{u_r^{n+\frac{1}{2}}-u_r^n}{\Delta\tau} = \Lambda_{4\varphi}^{[r]}u_r^{n+\frac{1}{2}}+\Lambda_{4r}^{[r]}u_r^n+\mathcal{N}_{[r]}^n\,, \quad (4.14)$$

$$\frac{u_r^{n+1}-u_r^{n+\frac{1}{2}}}{\Delta\tau} = \Lambda_{4r}^{[r]}(u_r^{n+1}-u_r^n)\,, \quad (4.15)$$

subjected to the respective boundary conditions.

The procedure of exclusion of the half-time step variable is the same.

It is clear that the boundary condition at the first half-time step $\Omega = 0$ is non-local which creates a problem when splitting is performed alongside the lines $\varphi = 0$ and $\varphi = \pi$. The said condition contains derivatives in both directions and hence it must also be splitted. So that, at the first half-time step we impose the splitted part of the condition, namely

$$\frac{u_r^{n+\frac{1}{2}}-u_r^n}{\Delta\tau} = \frac{1}{Re}\left(\Lambda_{\varphi\varphi}u_r^{n+\frac{1}{2}}+\Lambda_{rr}u_r^n\right) + \mathcal{L}^n[u_r] \quad (4.16)$$

$$\frac{u_r^{n+1}-u_r^{n+\frac{1}{2}}}{\Delta\tau} = \frac{1}{Re}\Lambda_{rr}(u_r^{n+1}-u_r^n), \quad (4.17)$$

where

$$\mathcal{L}[u_r] = -u_r\frac{\partial u_r}{\partial r} - \frac{\partial p}{\partial r} - \frac{1}{Re}\left(\frac{u_r}{r^2} + \frac{2}{r^2}\frac{\partial u_\varphi}{\partial \varphi}\right) .$$

The first of these conditions couples the b.v.p for u_φ on the first half–time step. On the second half-time step we use the second half-time step from the splitted version of the boundary condition which is to be considered as an one-dimensional difference parabolic equation solved under the following b.c.

$$u_r(1,\varphi) = 0 , \quad \frac{\partial u_r}{\partial r}(1,\varphi) = 0 ,$$

$$u_r(R_\infty,\varphi) = \cos\varphi , \quad \frac{\partial u_r}{\partial r}(R_\infty,\varphi) = 0 .$$

4.1.3. Splitting for p:

The splitting scheme for pressure reads:

$$\frac{p^{n+\frac{1}{2}} - p^n}{\Delta\tau} = \Lambda_{rr}p^{n+\frac{1}{2}} + \Lambda_{\varphi\varphi}p^n + \mathcal{N}^n_{[p]} \qquad (4.18)$$

$$\frac{p^{n+1} - p^{n+\frac{1}{2}}}{\Delta\tau} = \Lambda_{\varphi\varphi}(p^{n+1} - p^n), \qquad (4.19)$$

The boundary conditions that couple the three-diagonal systems for pressure are (3.9).

4.2. The Grid Pattern

In the present paper we employ only uniform meshes in both directions. The number of grid lines in the two directions are given respectively by N_r and N_φ. In order to secure second order of approximation of b.c. we use additional lines outside the domain under consideration (see Fig. 1) where the thick lines represent the borders of the region of computations). The spacings are then given by:

$$h_r = \frac{r_\infty - a}{N_r - 3} , \quad h_\varphi = \frac{\pi}{N_\varphi - 3} .$$

4.3. Difference Approximations for Equations

We use the standard central three-point differences for the first and second derivatives

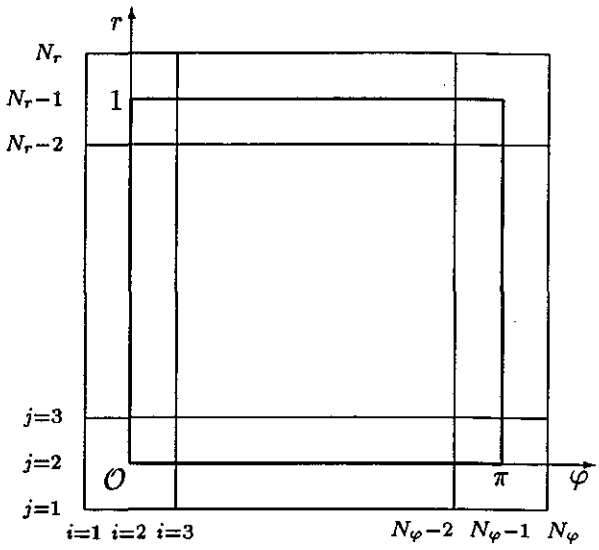

Figure 1: Grid pattern

and five-point central differences for the fourth derivatives, namely

$$\left.\frac{\partial u}{\partial x}\right|_i \simeq \frac{1}{2h}(u_{i+1} - u_{i-1})$$

$$\left.\frac{\partial^2 u}{\partial x^2}\right|_i \simeq \frac{1}{2h}(u_{i+1} - 2u_i + u_{i-1})$$

$$\left.\frac{\partial}{\partial x}w^2\frac{\partial u}{\partial x}\right|_i \simeq \frac{1}{h^2}\left[w^2_{i+\frac{1}{2}}u_{i+1} + w^2_{i-\frac{1}{2}}u_{i-1} - (w^2_{i+\frac{1}{2}} + w^2_{i-\frac{1}{2}})u_i\right] ,$$

where $w^2_{i+\frac{1}{2}} = (w_{i+1} + w_i)^2/4 ,$

$$\left.\frac{\partial}{\partial x}w\frac{\partial u}{\partial x}\right|_i \simeq \frac{1}{h^2}\left[w_{i+\frac{1}{2}}u_{i+1} + w_{i-\frac{1}{2}}u_{i-1} - (w_{i+\frac{1}{2}} + w_{i-\frac{1}{2}})u_i\right] ,$$

where $w_{i+\frac{1}{2}} = (w_{i+1} + w_i)/2 ,$

$$\left.\frac{\partial^4 u}{\partial x^4}\right|_i \simeq \frac{1}{h^4}(u_{i-2} - 4u_{i-1} + 6u_i - 4u_{i+1} + u_{i+2}) ,$$

$$\left.\frac{\partial^3 u}{\partial x^3}\right|_i \simeq \frac{1}{2h^3}(-u_{i-2} + 2u_{i-1} - 2u_{i+1} + u_{i+2}) ,$$

where u stands for u_r, u_φ or p, and x stands for

r or φ. Respectively h is either h_r or h_φ, and w denotes either u_φ^2 or $(u_r - \frac{1}{rRe})^2$.

The mixed (oblique) derivatives are approximated as follows

$$\frac{\partial^2 u}{\partial\varphi\partial r} \simeq \frac{1}{4h_\varphi h_r}(u_{i+1j+1} - u_{i+1j-1} - u_{i-1j+1} + u_{i-1j-1}) ,$$

$$\frac{\partial^3 u}{\partial\varphi\partial r^2} \simeq \frac{1}{2h_\varphi h_r^2}[(u_{i+1j+1} - 2u_{i+1j} + u_{i+1j-1}) - (u_{i-1j+1} - 2u_{i-1j} + u_{i-1j-1})] ,$$

$$\frac{\partial^3 u}{\partial r\partial\varphi^2} \simeq \frac{1}{2h_r h_\varphi^2}[(u_{i+1j+1} - 2u_{ij+1} + u_{i-1j+1}) - (u_{i+1j-1} - 2u_{ij-1} + u_{i-1j-1})] .$$

4.4. Difference Approximations for Boundary Conditions

The additional lines that were introduced in the grid (see Fig. 1) allow us to use central differences for the b.c. *First*, this makes the cheapest way to second-order approximation. *Second*, the approximation of b.c. is consistent with the approximation of equations. This has a positive effect upon the practical conservativeness of the scheme and increases the stability of iterations.

For function u_φ the boundary conditions are approximated as follows:

$$\begin{aligned}
r = 1 \quad &: \quad u_\varphi|_{i,2} = 0 , \quad \Phi_{i2} = 0 , \\
r = R_\infty \quad &: \quad u_\varphi|_{i,N_r-1} = -\sin\varphi_i , \\
&\quad\quad u_\varphi|_{i,N_r} - u_\varphi|_{i,N_r-2} = 0 , \\
\varphi = 0 \quad &: \quad u_\varphi|_{2,j} = 0 , \quad u_\varphi|_{1,j} + u_\varphi|_{3,j} = 0 , \\
\varphi = \pi \quad &: \quad u_\varphi|_{N_\varphi-1,j} = 0 , \\
&\quad\quad u_\varphi|_{N_\varphi-2,j} + u_\varphi|_{N_\varphi,j} = 0 ,
\end{aligned}$$

which closes the five-diagonal systems to which the half-time steps (4.10) and (4.11) are reduced.

For function u_r the b.c. are approximated as follows.

For $\varphi = 0, \pi$ at the first half-time step are used the conditions

$$u_r|_{1,j} - u_r|_{3,j} = u_r|_{N_\varphi-2,j} - u_r|_{N_\varphi,j} = 0 ,$$

and the equation (4.16) at $i = 2, N_\varphi - 1$. At the second half-time step the equation (4.17) is solved.

Respectively

$$\begin{aligned}
r = 1 \quad &: \quad u_r|_{i,2} = 0 , \quad u_r|_{i,3} - u_r|_{i,1} = 0 , \\
r = R_\infty \quad &: \quad u_r|_{i,N_r-1} = \cos\varphi_i , \\
&\quad\quad u_r|_{i,N_r} - u_r|_{i,N_r-2} = 0 ,
\end{aligned}$$

and thus the five-diagonal systems to which reduce (4.14) and (4.15) are closed.

All the above approximations for boundary conditions are of second spatial order.

Then the conditions on function $p(r,\varphi)$ can be approximated with second order too. The latter gives three-point differences at the boundaries which is not convenient for the three-diagonal systems (4.18) and (4.19) for $p(r,\varphi)$ at each half-time step. In order to close the system we perform the following.

For $r = 1$ from the natural condition of minimization of a functional we get

$$p|_{i,3} - p|_{i,1} = \frac{2}{h_r Re}(u_r|_{i,1} + u_r|_{i,3})$$

where is acknowledged that $u_r|_{2,2} = 0$. From eq.(4.18) taken at $j = 2$ we exclude $p|_{i,3}$ to obtain a two-point relation between $p|_{i,1}$ and $p|_{i,2}$.

In the same manner at $r = R_\infty$ we get from the respective N–S equation

$$p|_{i,N_r} - p|_{i,N_r-2} =$$

$$\frac{2}{h_r Re}(u_r|_{i,N_r-2} - 2u_r|_{i,N_r-1} + u_r|_{i,N_r}) ,$$

and from the eq.(4.18) taken at $j = N_r - 1$ we exclude $p|_{i,N_r-2}$ to obtain a two-point relation only involving $p|_{i,N_r}$ and $p|_{i,N_r-1}$.

In the same manner one can treat the b.c. for $\varphi = 0$, i.e., to exclude $p_{3,j}$ from

$$p|_{1,j} - p|_{3,j} = 0 ,$$

and from eq.(4.19) the latter taken at $i = 2$. Thus we a two-point relation only involving $p|_{1,j}$ and $p|_{2,j}$ is obtained.

In a similar fashion for $\varphi = \pi$ the value $p|_{N_\varphi-2,j}$ is excluded from

$$p|_{N_\varphi-2,j} - p|_{N_\varphi,j} = 0$$

and from the eq.(4.19) the latter taken at $i = N_\varphi - 1$.

4.5. Note on Solver Used

The splitting scheme reduces at each half-time step to five- or three- diagonal systems of algebraic equations. These are solved by the method of so-called non-monotonous progonka (see [5]) which is a kind of Gaussian elimination with pivoting that is highly efficient for multidiagonal cases.

4.6. Initial Conditions

The initial conditions for the different unknowns u_φ, u_r and p for small Reynolds numbers ($Re \approx 2 \div 4$) are defined as

$$u_\varphi|_{i,j} = \frac{r_j - 1}{r_\infty - 1}\cos\varphi_i\,, \tag{4.20}$$

$$u_r|_{i,j} = \frac{r_j - 1}{r_\infty - 1}\sin\varphi_i\,, \tag{4.21}$$

$$p|_{i,j} = 0\,, \tag{4.22}$$

$$\text{for} \qquad 1 \le i \le N_\varphi, \quad 1 \le j \le N_r,$$

For larger values of Reynolds number the solution for the closest smaller Re is used as the initial condition for the iterations for the current Re.

4.7. Calculating Stream Function

The problem under consideration is stationary and the stream lines coincide with the trajectories of the fluid particles. Hence the most convenient visualization of the flow are the isolines of the stream function. For this reason we calculate the stream function after the velocity components (u_r and u_φ) are obtained. It is known that the stream function Ψ is defined as

$$\frac{\partial\Psi}{\partial r} = u_\varphi\,, \quad \frac{\partial\Psi}{\partial\varphi} = -ru_r, \tag{4.23}$$

and satisfies the Poisson equation

$$\Delta\Psi = \omega \equiv \frac{\partial u_\varphi}{\partial r} + \frac{u_\varphi}{r} - \frac{1}{r}\frac{\partial u_r}{\partial\varphi}\,, \tag{4.24}$$

Boundary conditions for Ψ are obtained from (4.23) and the respective b.v.p. is a Neumann problem. It is clear that in our case due to the symmetries of the problem, we can use also the following Dirichlet conditions

$$\begin{aligned} &\Psi = 0 \quad \text{for} \quad r = 1\,,\ \varphi = 0, \pi\,, \\ &\Psi \to -r\sin\varphi \quad \text{for} \quad r \to \infty\,. \end{aligned} \tag{4.25}$$

There exists a plethora of different ways to solve the elliptic equation (4.24). Once again we employ the splitting method which in this case is the same as for the pressure equation. For this reason we will not discuss it here. We are only to mention here that for the linear Poisson equation the splitting scheme is unconditionally stable.

5. General Consequence of Algorithm

We solve the system governing the functions $u_\varphi(r,\varphi), u_r(r,\varphi)$ and $p(r,\varphi)$ in the following iterational manner:

(i) The initial conditions u^0_φ, u^0_r, p^0 are specified according to Subsection 4.6. The counter of time steps is set $n = 0$;

(ii) Setting $\hat{u}_r \equiv u^n_r$, $\hat{u}_\varphi \equiv u^n_\varphi$ and $\hat{p} \equiv p^n$, function u^{n+1}_φ is calculated from the respective equation;

(iii) Setting $\hat{u}_\varphi \equiv u^{n+1}_\varphi$, function u^{n+1}_r is calculated from the respective equation;

(iv) Setting $\hat{u}_r \equiv u^{n+1}_r$, function p^{n+1} is calculated from the respective equation.

(v) The norm of the difference between two consecutive iterations $(n+1)$ and (n) (time steps with respect to fictitious time) is calculated. If this norm is lesser than a prior prescribed value then the calculations are terminated. Otherwise the index of iterations is stepped up $n = n + 1$ and the algorithm is returned to step (ii).

6. Results and Discussion

The flow about a cylinder is an outer flow and this poses hard difficulties connected with the geometry. Since we are concerned in this first paper on the subject mostly by the problem of existence of solution for the imbedding problem, we do not employ non–uniform meshes, etc. Hence our computations are subject to the obvious limitations connected with the fact that the wake increases with Re approximately as the first power of Re. Note that the problem of the wake is still a subject of intensive investigations, especially for very large Re. When we speak for linear dependence on Re we are aware that it is approximately the case only for $Re < 100$. Anyway, it is restrictive enough and forces us to use more than 500 grid intervals in radial direction for the higher Reynolds numbers $Re \geq 80$.

The first, and the most significant result is, that one can indeed obtain a solution of the original N–S problem from the Imbedding b.v.p. This is an algorithmic verification of the statement that the solution of the original problem is among of the solutions of the Imbedding problem. Moreover, we did not actually encounter other solutions of Euler–Lagrange equations that give another local minimum of the Imbedding functional (3.1) rather than the solution of original N–S problem. It is clear that to formally prove this statement is a hard task, but our results are at least suggestive that if there exist more than one solution, then these solutions (attractors) are well separated in the functional space and starting from "reasonable" initial condition, we inevitably end up with the solution of the original problem after the iterations converge. One should be reminded that this is not the case with MVI applications to identification of homoclinics ([1,10]) where the gist of regularization consists in smooth transition from easily calculated "artificial" solution of the Imbedding problem with non–zero value for the functional, to the solution of the original one with zero value functional.

The highest Re for which we could get results on uniform grids without intolerable deformation of the solution was $Re = 100$. Fig. 2 shows the patterns of flow for different Reynolds numbers $Re \geq 30$ when the separation of the streaming is well established.

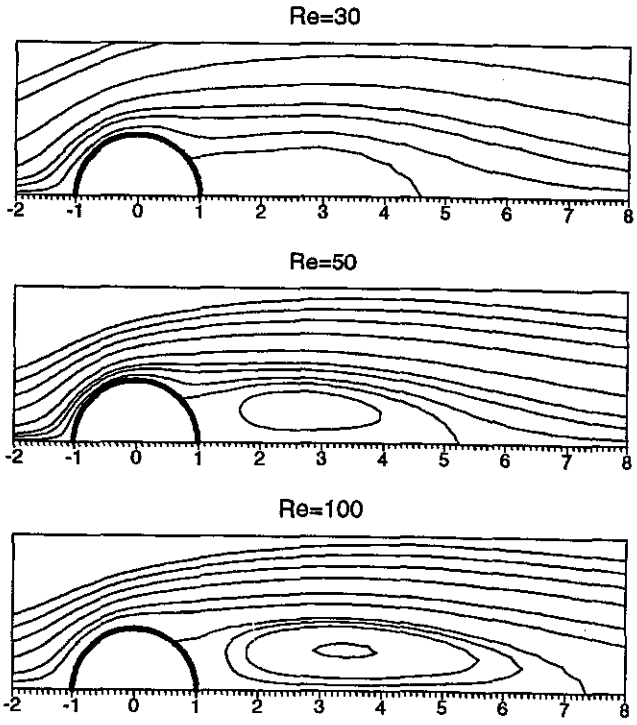

Figure 2: Streamlines the flow past a cylinder. Evolution with Reynolds number.

Respectively Fig. 3 presents the topography of the vorticity function for the largest Reynolds number $Re = 100$.

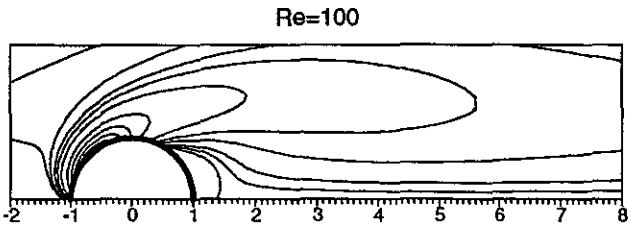

Figure 3: Vorticity isolines for $Re = 100$.

Important characteristics of the flow are the pressure and vorticity distributions alongside the cylinder surface. Fig. 4 shows the pressure distribution for different Reynolds number. It is seen

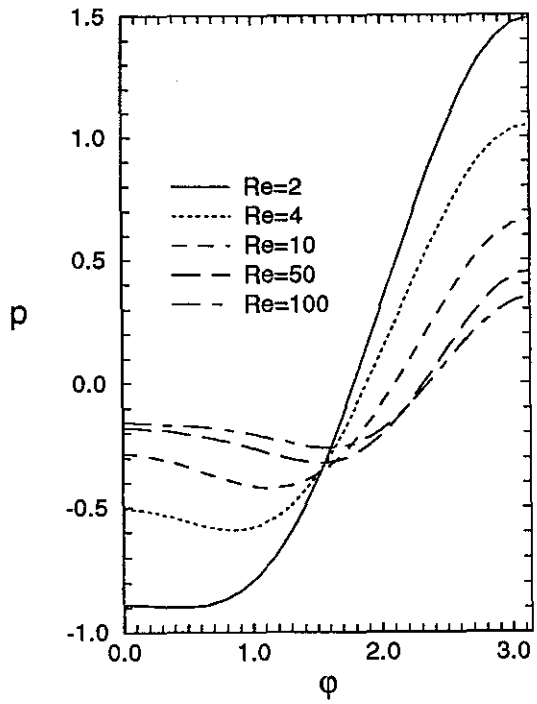

Figure 4: Pressure distribution along the surface of cylinder.

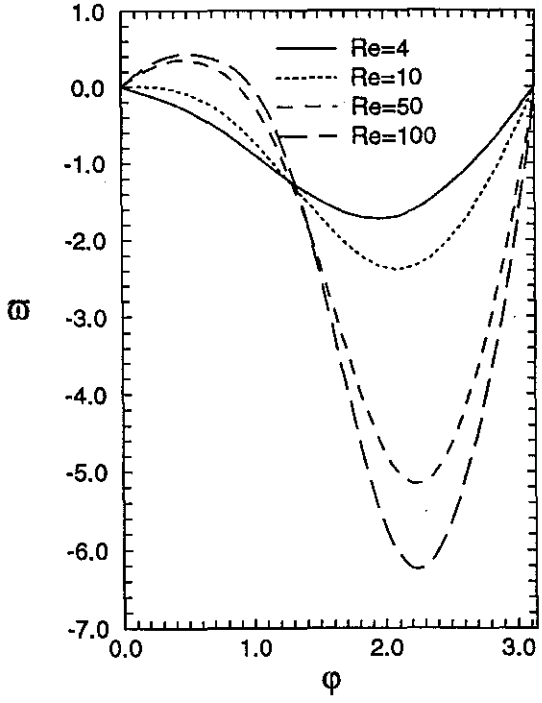

Figure 5: Distribution of vorticity function ω along the surface of cylinder.

that when $Re \geq 30$ the pressure distribution is quantitatively quite close to one of an ideal flow with separation.

Fig. 5 shows the vorticity distribution. Once again one sees that $Re \geq 30$ is already the range when the Reynolds number ceases to play quantitative role.

Quantitative comparison with the numerical calculations from the literature ensures that indeed the solution to the original N–S problem is obtained. With this the programme of the present work is fulfilled.

7. Conclusions

The steady solution to Navier–Stokes equations for high–Reynolds number is unstable to and hence the problem of its calculation is incorrect in the sense of Hadamard. Finding the steady solution to the problem around circular cylinder is considered here as an inverse problem and treated by the Method of Variational Imbedding (MVI). The original unstable problem is replaced by a higher–order boundary value problem for the Euler–Lagrange equations representing the necessary conditions for minimization of the square functional of the Navier–Stokes equations. For the numerical solution of the higher–order system a difference scheme of splitting type is devised and respective iterative algorithm is created. The performance of the scheme is verified on different uniform meshes. Results are obtained for $Re \leq 100$. This answers in affirmative the question of whether the steady solution does exist for Reynolds numbers $Re > 40$ when it ceases to be stable and the direct simulations of the time–dependent N–S fail to recover it. The pressure distribution and drag force compare quantitatively very well with the available experimental or numerical data.

References

[1] C. I. Christov. A method for identification of homoclinic trajectories. In *Proc. 14-th Spring Conf, Sunny Beach*, pages 571–577, Union of Bulg. Mathematicians, Sofia,Bulgaria, 1985.

[2] C. I. Christov. Method of variational imbedding for elliptic incorrect problems. *Comp. Rend. Acad. Buld. Sci.*, 39(12):23–26, 1986.

[3] C. I. Christov. The method of variational imbedding for parabolic incorrect problems of coefficient identification. *Comp. Rend. Acad. Buld. Sci.*, 40(2):21–24, 1987.

[4] C. I. Christov. The method of variational imbedding for time reversal incorrect parabolic problems. *Comp. Rend. Acad. Buld. Sci.*, 40(6):5–8, 1987.

[5] C. I. Christov. *Gaussian elimination with pivoting for multidiagonal systems.* University of Reading, Internal Report 4, 1994.

[6] C. I. Christov, J. Pontes, D. Walgraef, and M. G. Velarde. Implicit time splitting for fourth–order parabolic equations. *Computer Methods of Appl. Mech. Engineering*, 1994. (accepted)

[7] C. I. Christov and A. Ridha. Splitting scheme for iterative solution of bi- harmonic equation. application to 2D Navier–Stokes problems. In I. Dimov et al., editor, *Advances in Numerical Methods and Applications*, pages 341–352, World Scientific, Singapore, 1994.

[8] C. I. Christov and M. D. Todorov. An inviscid model of flow separation around blunt bodies. *Compt. Rend. Acad. Bulg. Sci.*, 7:43–46, 1987.

[9] C. I. Christov and M. D. Todorov. On the determination of the shape of stagnation zone in separated inviscid flows around blunt bodies. In *Proc. XV Jubilee Session on Ship Hydrodynamics, Varna, 1986*, page paper 10, BSHC, Varna, 1986.

[10] C. I. Christov and M. G. Velarde. On localized solutions of an equation governing Bénard-Marangoni convection. *Appl. Math. Modelling*, 17:311–320, 1993.

[11] S. C. R. Dennis and G. Z. Chang. Numerical solutions for steady flow past a circular cylinder at reynolds numbers up to 100. *J. Fluid Mech.*, 42:471–489, 1970.

[12] B. Fornberg. A numerical study of steady viscous flow past a circular cylinder. *J. Fluid Mech.*, 98:819–855, 1980.

[13] B. Fornberg. Steady viscous flow past a circular cylinder up to reynolds number 600. *J. Comput. Phys.*, 61:297–320, 1985.

[14] P. C. Jain and M. Kawaguti. Numerical study of viscous flow past circular cylinders. *J. Phys. Soc. Japan*, 21:2005–, 1966.

[15] P. C. Jain and K. Sankara Rao. Numerical soution of unsteady viscous incompressible fluid flow past a circular cylinder. *Phys. Fluids Supl.*, II:57–, 1969.

[16] M. Kawaguti. Numerical solution of the Navier–Stokes equations for the flow around a circular cylinder at reynolds number 40. *J. Phys. Soc. Japan*, 8:747–757, 1953.

[17] H. B. Keller and H. Takami. Numerical studies of viscous flow about cylinders. In D. Greenspan, editor, *Numerical Solutions of Nonlinear Differential Equations*, pages 115–, Wiley, 1966.

[18] R. S. Marinova and C. I. Christov. Numerical investigation of the stationary 2D flow around cylinder by means of Method of Variational Imbedding. In *Proc. 18th National Summer School on Applications of Mathematics, Varna 25.08-02.09.92*, pages 162-165, Sofia, 1993.

[19] T. Marinov and C. Christov. Boundary layer thickness as an inverse problem of coefficient identification. In *HADMAR'91, Varna, Bulgaria*, page 57, Bulgarian Institute of Ship Hydrodynamics, Varna, 1994.

[20] F. Nieuwshtadt and H. B. Keller. Viscous flow past cylinders. *Comp. Fluids*, 1:59–, 1973.

[21] V. A. Patel. Symmetry of the flow around a circular cylinder. *J. Comp. Phys.*, 71:65–99, 1987.

[22] D. W. Peaceman and Jr. H. H. Rachford. The numerical solution of parabolic and elliptic differential equations. *J. Soc. Indust. Appl. Math.*, 3(No 1):28–41, 1955.

[23] J. S. Son and T. J. Hanratty. Numerical solution for the flow around a cylinder at reynolds number 40, 200, 500. *J. Fluid Mech.*, 35:369–386, 1969.

[24] P. L. Ta. Étude numérique de l'écoulement d'un fluide viscueux incompressible autour d'un cylindre fixe ou en rotation. effet magnus. *J. Mecanique*, 14:109–, 1975.

[25] H. Takami and H. B. Keller. Steady two–dimensional viscous flow of an incompressible fluid past a circular cylinder. *Phys. Fluids Suppl.*, II:51–, 1969.

[26] A. Thom. The flow past cyrcular cylinder at low speeds. *Proc. Roy. Soc.*, A 141:651–, 1933.

[27] D. C. Thoman and A. A. Szewczyk. Time dependent viscous flow over a circular cylinder. *Phys. Fluids Suppl.*, II:76–, 1969.

[28] S. Y. Tuann and M. D. Olson. Numerical studies of the flow around a circular cylinder by a finite element method. *Comp. Fluids*, 6:219, 1978.

[29] R. L. Underwood. Calculations of incompressible flow past a circular cylinder at moderate reynolds numbers. *J. Fluid Mech.*, 37:95–, 1969.

[30] N. N. Yanenko. *Method of Fractional Steps.* Gordon and Breach, 1971.

8. Appendix: Euler-Lagrange Equations

For u_φ:

$$\left(\frac{2u_\varphi}{r}-\frac{1}{r}\frac{\partial u_\varphi}{\partial\varphi}\right)\left[u_r\frac{du_r}{dr}+\frac{u_\varphi}{r}\frac{du_r}{d\varphi}-\frac{u_\varphi^2}{r}+\frac{dp}{dr}--\frac{1}{Re}\left(\frac{\partial^2u_r}{\partial r^2}+\frac{1}{r}\frac{\partial u_r}{\partial r}+\frac{1}{r^2}\frac{\partial^2u_r}{\partial\varphi^2}-\frac{u_r}{r^2}-\frac{2}{r^2}\frac{\partial u_\varphi}{\partial\varphi}\right)\right]$$

$$-\left(\frac{1}{r}\frac{\partial u_\varphi}{\partial\varphi}+\frac{2}{r^2Re}\right)\left[u_r\frac{du_\varphi}{dr}+\frac{u_\varphi}{r}\frac{du_\varphi}{d\varphi}+\frac{u_\varphi u_r}{r}+\frac{1}{r}\frac{\partial p}{\partial\varphi}-\frac{1}{Re}\left(\frac{\partial^2u_\varphi}{\partial r^2}+\frac{1}{r}\frac{\partial u_\varphi}{\partial d}+\frac{1}{r^2}\frac{\partial^2u_\varphi}{\partial\varphi^2}-\frac{u_\varphi}{r^2}+\frac{2}{r^2}\frac{\partial u_r}{\partial\varphi}\right)\right]$$

$$+\frac{\partial}{\partial r}\left\{\left(u_r-\frac{1}{Re}\right)\left[u_r\frac{\partial u_\varphi}{\partial r}+\frac{u_\varphi}{r}\frac{\partial u_\varphi}{\partial\varphi}+\frac{u_\varphi u_r}{r}+\frac{1}{r}\frac{\partial p}{\partial\varphi}-\frac{1}{Re}\left(\frac{\partial^2u_\varphi}{\partial r^2}+\frac{1}{r}\frac{\partial u_\varphi}{\partial r}+\frac{1}{r^2}\frac{\partial^2u_\varphi}{\partial\varphi^2}-\frac{u_\varphi}{r^2}+\frac{2}{r^2}\frac{\partial u_r}{\partial\varphi}\right)\right]\right\}$$

$$+\frac{2}{r\,Re}\frac{\partial}{\partial r}\left[u_r\frac{\partial u_\varphi}{\partial r}+\frac{u_\varphi}{r}\frac{\partial u_\varphi}{\partial\varphi}+\frac{u_\varphi u_r}{r}+\frac{1}{r}\frac{\partial p}{\partial\varphi}--\frac{1}{Re}\left(\frac{\partial^2u_\varphi}{\partial r^2}+\frac{1}{r}\frac{\partial u_\varphi}{\partial r}+\frac{1}{r^2}\frac{\partial^2u_\varphi}{\partial\varphi^2}-\frac{u_\varphi}{r^2}+\frac{2}{r^2}\frac{\partial u_r}{\partial\varphi}\right)\right]$$

$$+\frac{1}{r}\frac{\partial}{\partial\varphi}\left\{u_\varphi\left[u_r\frac{\partial u_\varphi}{\partial r}+\frac{u_\varphi}{r}\frac{\partial u_\varphi}{\partial\varphi}+\frac{u_\varphi u_r}{r}+\frac{1}{r}\frac{\partial p}{\partial\varphi}-\frac{1}{Re}\left(\frac{\partial^2u_\varphi}{\partial r^2}+\frac{1}{r}\frac{\partial u_\varphi}{\partial r}+\frac{1}{r^2}\frac{\partial^2u_\varphi}{\partial\varphi^2}-\frac{u_\varphi}{r^2}+\frac{2}{r^2}\frac{\partial u_r}{\partial\varphi}\right)\right]\right\}$$

$$+\frac{2}{r^2\,Re}\frac{\partial}{\partial\varphi}\left[u_r\frac{\partial u_r}{\partial r}+\frac{u_\varphi}{r}\frac{\partial u_r}{\partial\varphi}-\frac{u_\varphi^2}{r}+\frac{\partial p}{\partial r}-\frac{1}{Re}\left(\frac{\partial u_r}{\partial r}+\frac{1}{r}\frac{\partial u_r}{\partial r}+\frac{1}{r^2}\frac{\partial^2u_r}{\partial\varphi^2}-\frac{u_r}{r^2}-\frac{2}{r^2}\frac{\partial u_\varphi}{\partial\varphi}\right)\right]$$

$$+\frac{1}{Re}\frac{\partial^2}{\partial r^2}\left[u_r\frac{\partial u_\varphi}{\partial r}+\frac{u_\varphi}{r}\frac{\partial u_\varphi}{\partial\varphi}+\frac{u_\varphi u_r}{r}+\frac{1}{r}\frac{\partial p}{\partial\varphi}-\frac{1}{Re}\left[\frac{\partial^2u_\varphi}{\partial r^2}+\frac{1}{r}\frac{\partial u_\varphi}{\partial r}+\frac{1}{r^2}\frac{\partial^2u_\varphi}{\partial\varphi^2}-\frac{u_\varphi}{r^2}+\frac{2}{r^2}\frac{\partial u_r}{\partial\varphi}\right)\right]$$

$$+\frac{1}{r^2Re}\frac{\partial^2}{\partial\varphi^2}\left[u_r\frac{\partial u_\varphi}{\partial r}+\frac{u_\varphi}{r}\frac{\partial u_\varphi}{\partial\varphi}+\frac{u_\varphi u_r}{r}+\frac{1}{r}\frac{\partial p}{\partial\varphi}-\frac{1}{Re}\left(\frac{d^2u_\varphi}{dr^2}+\frac{1}{r}\frac{du_\varphi}{dr}+\frac{1}{r^2}\frac{d^2u_\varphi}{d\varphi^2}-\frac{u_\varphi}{r^2}+\frac{2}{r^2}\frac{du_r}{d\varphi}\right)\right]$$

$$+\frac{1}{r}\frac{d}{d\varphi}\left(\frac{du_r}{dr}+\frac{u_r}{r}+\frac{1}{r}\frac{du_\varphi}{d\varphi}\right) \tag{8.1}$$

For u_r:

$$-\left(\frac{\partial u_\varphi}{\partial r}+\frac{u_r}{r}\right)\left[u_r\frac{\partial u_\varphi}{\partial r}+\frac{u_\varphi}{r}\frac{\partial u_\varphi}{\partial\varphi}+\frac{u_\varphi u_r}{r}+\frac{1}{r}\frac{\partial p}{\partial\varphi}-\frac{1}{Re}\left(\frac{\partial^2u_\varphi}{\partial r^2}+\frac{1}{r}\frac{\partial u_\varphi}{\partial r}+\frac{1}{r^2}\frac{\partial^2u_\varphi}{\partial\varphi^2}-\frac{u_\varphi}{r^2}+\frac{2}{r^2}\frac{\partial u_r}{\partial\varphi}\right)\right]$$

$$-\left(\frac{\partial u_r}{\partial r}-\frac{u_r}{r}+\frac{2}{r^2Re}\right)\left[u_r\frac{\partial u_r}{\partial r}+\frac{u_\varphi}{r}\frac{\partial u_r}{\partial\varphi}-\frac{u_\varphi^2}{r}+\frac{\partial p}{\partial r}-\frac{1}{Re}\left(\frac{\partial^2u_r}{\partial r^2}+\frac{1}{r}\frac{\partial u_r}{\partial r}+\frac{1}{r^2}\frac{\partial^2u_r}{\partial\varphi^2}-\frac{u_r}{r^2}-\frac{2}{r^2}\frac{\partial u_\varphi}{\partial\varphi}\right)\right]$$

$$+\frac{\partial}{\partial r}\left\{\left(u_r-\frac{1}{r\,Re}\right)\left[u_r\frac{\partial u_r}{\partial r}+\frac{u_\varphi}{r}\frac{\partial u_r}{\partial\varphi}-\frac{u_\varphi^2}{r}+\frac{\partial p}{\partial r}-\frac{1}{Re}\left(\frac{\partial^2u_r}{\partial r^2}+\frac{1}{r}\frac{\partial u_r}{\partial r}+\frac{1}{r^2}\frac{\partial^2u_r}{\partial\varphi^2}-\frac{u_r}{r^2}-\frac{2}{r^2}\frac{\partial u_\varphi}{\partial\varphi}\right)\right]\right\}$$

$$+\frac{2}{r\,Re}\frac{\partial}{\partial r}\left[u_r\frac{\partial u_r}{\partial r}+\frac{u_\varphi}{r}\frac{\partial u_r}{\partial\varphi}-\frac{u_\varphi^2}{r}+\frac{\partial p}{\partial r}-\frac{1}{Re}\left(\frac{\partial^2u_r}{\partial r^2}+\frac{1}{r}\frac{\partial u_r}{\partial r}+\frac{1}{r^2}\frac{\partial^2u_r}{\partial\varphi^2}-\frac{u_r}{r^2}-\frac{2}{r^2}\frac{\partial u_\varphi}{\partial\varphi}\right)\right]$$

$$+\frac{1}{r}\frac{\partial}{\partial\varphi}\left\{u_\varphi\left[u_r\frac{\partial u_r}{\partial r}+\frac{u_\varphi}{r}\frac{\partial u_r}{\partial\varphi}-\frac{u_\varphi^2}{r}+\frac{\partial p}{\partial r}-\frac{1}{Re}\left(\frac{\partial^2 u_r}{\partial r^2}+\frac{1}{r}\frac{\partial u_r}{\partial r}+\frac{1}{r^2}\frac{\partial^2 u_r}{\partial\varphi^2}-\frac{u_r}{r^2}-\frac{2}{r^2}\frac{\partial u_\varphi}{\partial\varphi}\right)\right]\right\}$$

$$-\frac{2}{r^2 Re}\frac{\partial}{\partial\varphi}\left[u_r\frac{\partial u_\varphi}{\partial r}+\frac{u_\varphi}{r}\frac{\partial u_\varphi}{\partial\varphi}+\frac{u_\varphi u_r}{r}+\frac{1}{r}\frac{\partial p}{\partial\varphi}-\frac{1}{Re}\left(\frac{\partial^2 u_\varphi}{\partial r^2}+\frac{1}{r}\frac{\partial u_\varphi}{\partial r}+\frac{1}{r^2}\frac{\partial^2 u_\varphi}{\partial\varphi^2}-\frac{u_\varphi}{r^2}+\frac{2}{r^2}\frac{\partial u_r}{\partial\varphi}\right)\right]$$

$$+\frac{1}{Re}\frac{\partial^2}{\partial r^2}\left[u_r\frac{\partial u_r}{\partial r}+\frac{u_\varphi}{r}\frac{\partial u_r}{\partial\varphi}-\frac{u_\varphi^2}{r}+\frac{\partial p}{\partial r}-\frac{1}{Re}\left(\frac{\partial^2 u_r}{\partial r^2}+\frac{1}{r}\frac{\partial u_r}{\partial r}+\frac{1}{r^2}\frac{\partial^2 u_r}{\partial\varphi^2}-\frac{u_r}{r^2}-\frac{2}{r^2}\frac{\partial u_\varphi}{\partial\varphi}\right)\right]$$

$$+\frac{1}{r^2 Re}\frac{\partial^2}{\partial\varphi^2}\left[u_r\frac{\partial u_r}{\partial r}+\frac{u_\varphi}{r}\frac{\partial u_r}{\partial\varphi}-\frac{u_\varphi^2}{r}+\frac{\partial p}{\partial r}-\frac{1}{Re}\left(\frac{\partial^2 u_r}{\partial r^2}+\frac{1}{r}\frac{\partial u_r}{\partial r}+\frac{1}{r^2}\frac{\partial^2 u_r}{\partial\varphi^2}-\frac{u_r}{r^2}-\frac{2}{r^2}\frac{\partial u_\varphi}{\partial\varphi}\right)\right]\cdot$$

$$+\frac{\partial}{\partial r}\left(\frac{\partial u_r}{\partial dr}+\frac{u_r}{r}+\frac{1}{r}\frac{\partial u_\varphi}{\partial\varphi}\right) \tag{8.2}$$

For p:

$$\frac{\partial^2 p}{\partial r^2}+\frac{1}{r}\frac{\partial p}{\partial r}+\frac{1}{r^2}\frac{\partial^2 p}{\partial\varphi^2}+\frac{\partial}{\partial r}(u_r\frac{\partial u_r}{\partial r}+\frac{u_\varphi}{r}\frac{\partial u_r}{\partial\varphi}-\frac{u_\varphi^2}{r}) \tag{8.3}$$

$$+\frac{1}{r}(u_r\frac{\partial u_r}{\partial r}+\frac{u_\varphi}{r}\frac{\partial u_r}{\partial\varphi}-\frac{u_\varphi^2}{r})+\frac{1}{r}\frac{\partial}{\partial\varphi}(u_r\frac{\partial u_\varphi}{\partial r}+\frac{u_\varphi}{r}\frac{\partial u_\varphi}{\partial d\varphi}+\frac{u_\varphi u_r}{r})=0,$$

since

$$\frac{\partial}{\partial r}\left(\frac{\partial^2 u_r}{\partial r^2}+\frac{1}{r}\frac{\partial u_r}{\partial r}+\frac{1}{r^2}\frac{\partial^2 u_r}{\partial\varphi^2}-\frac{u_r}{r^2}-\frac{2}{r^2}\frac{\partial u_\varphi}{\partial\varphi}\right)+\frac{1}{r}\left(\frac{\partial^2 u_r}{\partial r^2}+\frac{1}{r}\frac{\partial u_r}{\partial r}+\frac{1}{r^2}\frac{\partial^2 u_r}{\partial\varphi^2}-\frac{u_r}{r^2}-\frac{2}{r^2}\frac{\partial u_\varphi}{\partial\varphi}\right)$$

$$+\frac{1}{r}\frac{\partial}{\partial\varphi}\left(\frac{\partial^2 u_\varphi}{\partial r^2}+\frac{1}{r}\frac{\partial u_\varphi}{\partial r}+\frac{1}{r^2}\frac{\partial^2 u_\varphi}{\partial\varphi^2}-\frac{u_\varphi}{r^2}+\frac{2}{r^2}\frac{\partial u_r}{\partial\varphi}\right)\equiv\left(\frac{\partial^2}{\partial r^2}+\frac{1}{r}\frac{\partial}{\partial r}+\frac{1}{r^2}\frac{\partial^2}{\partial\varphi^2}\right)\left(\frac{\partial u_r}{\partial r}+\frac{u_r}{r}+\frac{1}{r}\frac{\partial u_\varphi}{\partial\varphi}\right)=0\,.$$